Making adaptive optics available to all: a concept for 1m class telescopes

Olivier Lai, Stefan Kuiper, Niek Doelman, Mark Chun, Dirk Schmidt, Frantz Martinache, Marcel Carbillet, Mamadou N'Diaye, Jean-Pierre Rivet

Making adaptive optics available to all: a concept for 1m class telescopes.

Olivier Lai*[a], Stefan Kuiper[b], Niek J. Doelman[b,c], Mark Chun[d], Dirk Schmidt[e], Frantz Martinache[a], Marcel Carbillet[a], Mamadou N'Diaye[a], Jean Pierre Rivet[a]
[a]Université Côte d'Azur, Obs. de la Côte d'Azur, Laboratoire Lagrange, CNRS, 06000 Nice, France; [b]TNO, Leiden, The Netherlands; [c]Leiden Observatory, Leiden, the Netherlands, [d]Institute for Astronomy, University of Hawaii, 640 N. A'ohoku Place, Hilo, HI 96720, USA; [e]National Solar Observatory, 3665 Discovery Dr, Boulder, CO 80303, USA.

ABSTRACT

Adaptive optics is an advanced technique developed for large telescopes. It turns out to be challenging for smaller telescopes (0.5~2m) due to the small isoplanatic angle, small subapertures and high correction speeds needed at visible wavelengths, requiring bright stars for guiding, severely limiting the sky coverage. The motivation to develop compact and robust AO system for small telescopes is two-fold: On the one hand, schools and universities often have access to small telescopes as part of their education programs. Also, researchers in countries with fewer resources could also benefit from well-engineered and reliable adaptive optics on smaller telescopes for research and education purposes. On the other hand, amateur astronomers and enthusiasts want improved image quality for visual observation and astrophotography. Implementing readily accessible adaptive optics in astronomy clubs would also likely have a significant impact on citizen science.

Keywords: Telescopes, wide field imaging, high angular resolution, wavefront sensing, ground layer adaptive optics.

1. INTRODUCTION

Adaptive optics is an advanced technique which has been developed for large telescopes (e.g., Babcock, 1953 [2]; Roddier, 1999 [13]) using state of the art components (custom optics, deformable mirrors, high performance computers). A number of challenges have hindered our ability to apply this technology to smaller telescopes and for general use, especially for amateur telescopes and astrophotography. One of the challenges is that the atmospheric phase disturbances increase with decreasing wavelength, and most AO systems for large telescopes are optimised for the infrared domain. On a smaller telescope, some of the constraints are relaxed since the phase variance that must be corrected is proportional to $(D/r_0)^{5/3}$, where D is the telescope diameter and r_0 is the Fried parameter describing the size of a coherence zone on a wavefront degraded by atmospheric turbulence. Since r_0 is chromatic ($\propto \lambda^{1.2}$), an 8-meter telescope in K band (2.2 µm) requires approximately the same level of correction as a 1-meter telescope at 500 nm. Most amateur astronomers are more interested in visible wavelengths (e.g. most nebulas have their strongest emission lines in that part of the spectrum, commercially available large format CCD or CMOS cameras are sensitive at those wavelengths) but adaptive optics in the visible is challenging. For 1-2 m class telescopes, traditional AO (SCAO: single conjugate adaptive optics) imposes severe limitations for sky coverage:

- Due to the small physical size of the subapertures on the primary mirror and the high frame rate, the limiting magnitude is bound to be small (around 5~8, depending on the telescope diameter and the order of the system, see e.g., Loktev et al., 2008 [7] or more recently Dauvergne et al., 2018 [3]).
- Because the isoplanatic field is very small in the optical domain, the quality of the correction will rapidly decrease further away from the guide star. Therefore, the parts of the sky where adequate correction is possible are limited to tens of arcseconds around some thousands of bright stars or planets.

The sky coverage could potentially be increased with the use of Laser Guide Stars; however, for small telescopes this is problematic for two reasons: first, because the subapertures are small, the required laser power is bound to be large, and handling powerful lasers poses its own challenges from a practical standpoint. Second, although the cone effect (also called

focal anisoplanatism) is small for small telescopes and allows the use of Rayleigh beacons (which are simpler and cheaper than the Sodium LGS used on large telescopes), it is still a complex technology (with safety and operational constraints) and an added cost to any adaptive optics instrument.

Natural guide star (NGS) SCAO is ideal for planetary objects but remains limited for general purpose observing. In this study, we propose a new solution based on multiple recently developed concepts brought together to enable a whole new field of application.

1.1 Motivation to develop AO on 0.5-2m class telescopes

The gain in resolution and sensitivity (for sky background limited observations) is obviously more significant on large telescopes (being proportional to D/r_0 and $(D/r_0)^2$ respectively). This is the reason why most astronomical adaptive optics research has focused on large telescopes, requiring significant budgets and prototypal development. However, by reducing the technical complexity and the associated financial constraints we are able to open up whole new fields of applications on smaller telescopes. This potentially makes adaptive optics accessible to whole new communities, especially considering that there are many more telescopes in the 1-2m class than in the 8-10 m class (Zipf's law indicates that the rank is inversely proportional to the frequency, and this applies to telescopes! See Figure 1):

- On the one hand, schools and universities often have access to small telescopes as part of their education programs. Furthermore, researchers in countries with fewer resources would also benefit from well engineered and robust adaptive optics on smaller telescopes, by improving their performance and exposure to advanced optics.
- On the other hand, amateur astronomers and enthusiasts would be enthusiastic for improved image quality for visual observation and astrophotography. Implementing readily accessible adaptive optics in astronomy clubs would also likely have a significant impact on citizen science.

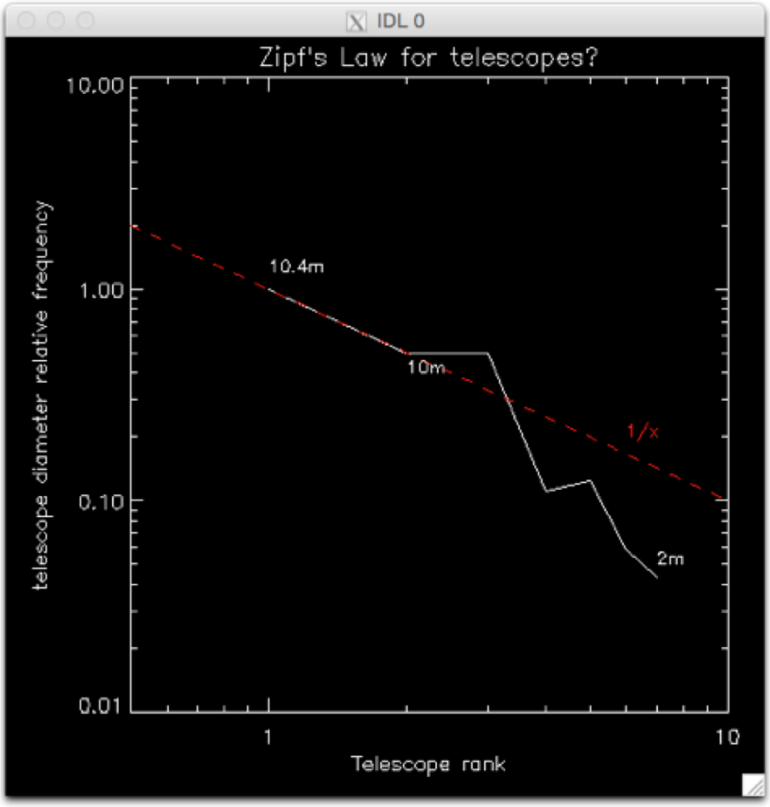

Figure 1: Zipf's law for telescopes (note that it becomes difficult to comprehensively identify all telescopes smaller than 2m globally)

2. CONCEPTUAL IMPLEMENTATION

2.1 GLAO

To enable large sky coverage we first recognize that we cannot correct the entire volume of turbulence above the telescope or in a direction where there is no source to illuminate the wavefront perturbation we are trying to correct. The next best thing we can do is to correct the turbulence which is common to the entire field we are trying to capture. This is achieved by the technique of GLAO (Ground Layer Adaptive Optics, e.g., Rigaut, 2002 [11], Tokovinin, 2004 [17]), whereby a single deformable mirror, conjugated as close to the telescope pupil as possible is used to correct only the ground layer turbulence. The latter is obtained by averaging wavefront measurements in multiple directions. In GLAO, the corrected wavefront will be limited by the residuals of the free atmosphere turbulence which are not corrected, so resulting images will in general not be diffraction limited but will show a substantial improvement in FWHM. This will depend on the vertical turbulence profile above the telescope and will be site-specific, but unless there are shears in the high atmosphere (e.g., jet stream), most sites are dominated by their boundary layers.

2.2 Optical differentiation Wavefront Sensor

To obtain an average wavefront in multiple directions normally requires as many wavefront sensors as there are sources in the field (Stuik et al, 2006 [16]; Abdurrahman et al., 2018 [1]), and this can become very costly, in terms of pixels, complexity (pickoffs) and obviously price. Since it is not possible to measure phase directly in the optical domain, a wavefront sensor usually uses an optical element to transform the phase object into a function of intensity, which we can measure. Usually the optical element is introduced in the pupil plane (e.g. lenslet array for a Shack-Hartmann generating the derivative of the phase) and the measurements are carried out in the focal plane. However another class of wavefront sensors exist where the optical operator is in the focal plane and the measurements are made in the pupil plane, such as Francois Roddier's curvature sensor (where a defocusing membrane mirror is placed in a focal plane and intensity measurements are carried out in the pupil plane, see Roddier, 1988 [12]), Roberto Ragazzoni's pyramid wavefront sensor (Ragazzoni, 1996 [9]), or the Optical Differentiation WFS (ODWFS, Schmidt & von der Lühe, 2007 [15]). A review of the principles of these so-called Fourier-based wavefront sensors can be found in Fauvarque et al, 2017 [4]. For wide field adaptive optics, there is an advantage to using the latter as all the light in the field can be averaged optically in the pupil, naturally producing an optimal measurement of the ground layer turbulence (we note in passing that this idea was first introduced by Roberto Ragazoni in his layer oriented MCAO concept, where the MCAO layers are reconstructed as a function of the size of the measurement field, see Ragazzoni et al., 2002 [10]). Further advantages include not requiring a laser beacon, as well as ease of acquisition (the constraints on the precise alignment between the guide star and the wavefront sensor are relaxed).

We have studied different focal plane filters, such as arrays of micro-pyramids or optical differentiation masks (optimised for edges and zones of strong intensity gradient), assuming our wavefront sensing scene is a random star field. We recognize that different sources may have different optimal masks and that it may be possible to use addressable masks (such as DMDs (digital micro-mirror devices), MEMS (micro-electrical mechanical systems) or LCD (liquid crystal display) screens) to adapt the focal plane optical filter for different scenes (the Moon, planets, galaxies), but random star fields offer the most versatility, especially if we favor the simplicity of a fixed focal plane optical operator. If the mask in the focal plane is fixed and we assume a random distribution of stars, the focal plane mask must include an asymmetry so that the signals from different stars do not cancel out.

For example, a possible focal plane optical operator could be an array of micropyramids; randomly positioned stars would obviously not fall at the apex of each pyramid, but if each star was not too far away from a pyramid's edge, it would contribute some signal to the high order wavefront, and for enough stars, the tip-tilt would average out. However, a micropyramid array also contains an anti-micropyramid array (where the positive pyramids meet, there are negative creases which act like anti-pyramids, see Figure 2) which cancel out (or worse, produce a non-linear mixture of) the signal.

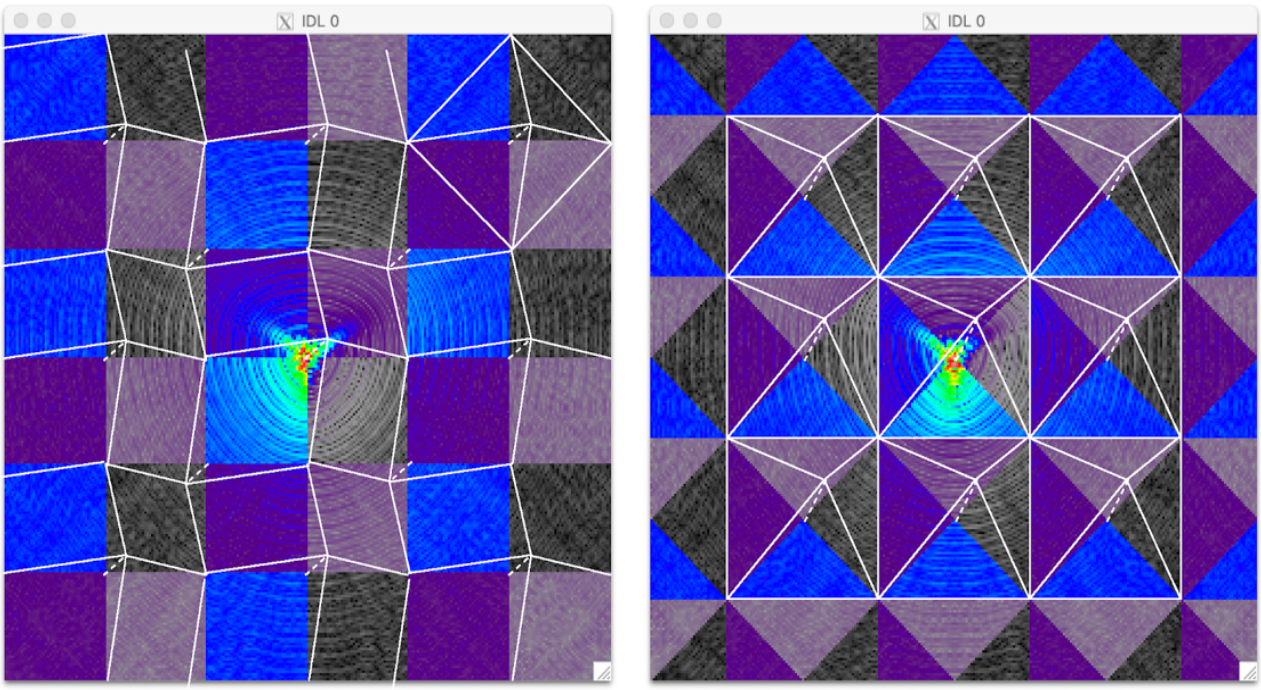

Figure 2: Left, Pyramid array with positive and negative pyramid and square facets. Although the array on the right appears to be made of only positive pyramids, there are still negative creases at their intersection producing an opposite sign signal.

Guided by S. Haffert' in depth study on generalised optical differentiation wavefront sensing (Haffert, 2016 [5]), we have empirically found that we obtain best results with an optical differentiation mask such as an array of continuous intensity ramps. The sharp jumps between each ramp act as a Foucault knife edge of the opposite sign as the gradual ramps, so we have developed an algorithm to position the mask such that the minimum amount of light falls near a sharp edge. On an actual system, this optimisation can be achieved by introducing a known phase (e.g., poke an actuator on the mirror) and slewing the telescope around until the signal of the phase on the wavefront sensor for that field is maximised. The number of ramps is still a free parameter in our concept as its optimal value depends on the field and the star count per unit area: sharper ramps (greater number of ramps per arcminute) provide a stronger gain on the signal but increase the probability that stars will be close to the sharp edges. We show an example using a random star field and different phase masks (low order Zernike and Kolmogorov turbulence phase screen) in Figure 3.

Another consideration is the size of the field over which the wavefront sensing can be carried out: the larger the field, the more light will be available for the wavefront sensor and the better the GLAO averaging. If the field is too small, there will be large variations in the corrected image quality as the optical averaging is done directly on the wavefront sensor, the contribution to the correction is weighted by the brightness of each star; one can see that the correction will be much more uniform if the field contains numerous stars of equal magnitude, as opposed to one very bright star.

However, a large field also means larger optics for reimaging the field into pupil images and there are also limits to the size of affordable science cameras (on the order of 10'). It may well be that different field sizes will be required for different telescopes and different projects; for example, a 1-m amateur telescope may not need a very large field, being more interested in crowded regions in the galactic plane, which will help reduce the cost, while a 2-m class professional telescope may favor 100% sky coverage with performance requirements at the North Galactic Pole, in which case a larger field will be necessary to collect more light. Note that nothing prevents this concept to be deployed over extremely large (>1˚) fields on 4m class or for routine GLAO wavefront sensing on 8-10m class telescopes (such as Gemini or Keck), but this is beyond the scope of the current study.

There is a definite trade-off between sensitivity/sky coverage and cost: Not only for the size of the field and the associated optics but also in design: it would be much simpler and cheaper to make a single image version of the optical differentiation wavefront sensor (using semi-reflective array of microramps), but half the light in the wavefront sensor would be lost. This

loss of sensitivity must be weighed against the applications and available budget, especially for smaller telescopes. However, to develop a proof-of-concept prototype, this may be an attractive solution. Another option might be to rotate the focal plane mask continuously and reconstruct the x- and y-derivatives by demodulating a synchronous detection, but the jumps at the sharp edges would cross every star in the field at some point, making this approach unusable for large fields requiring more than one ramp.

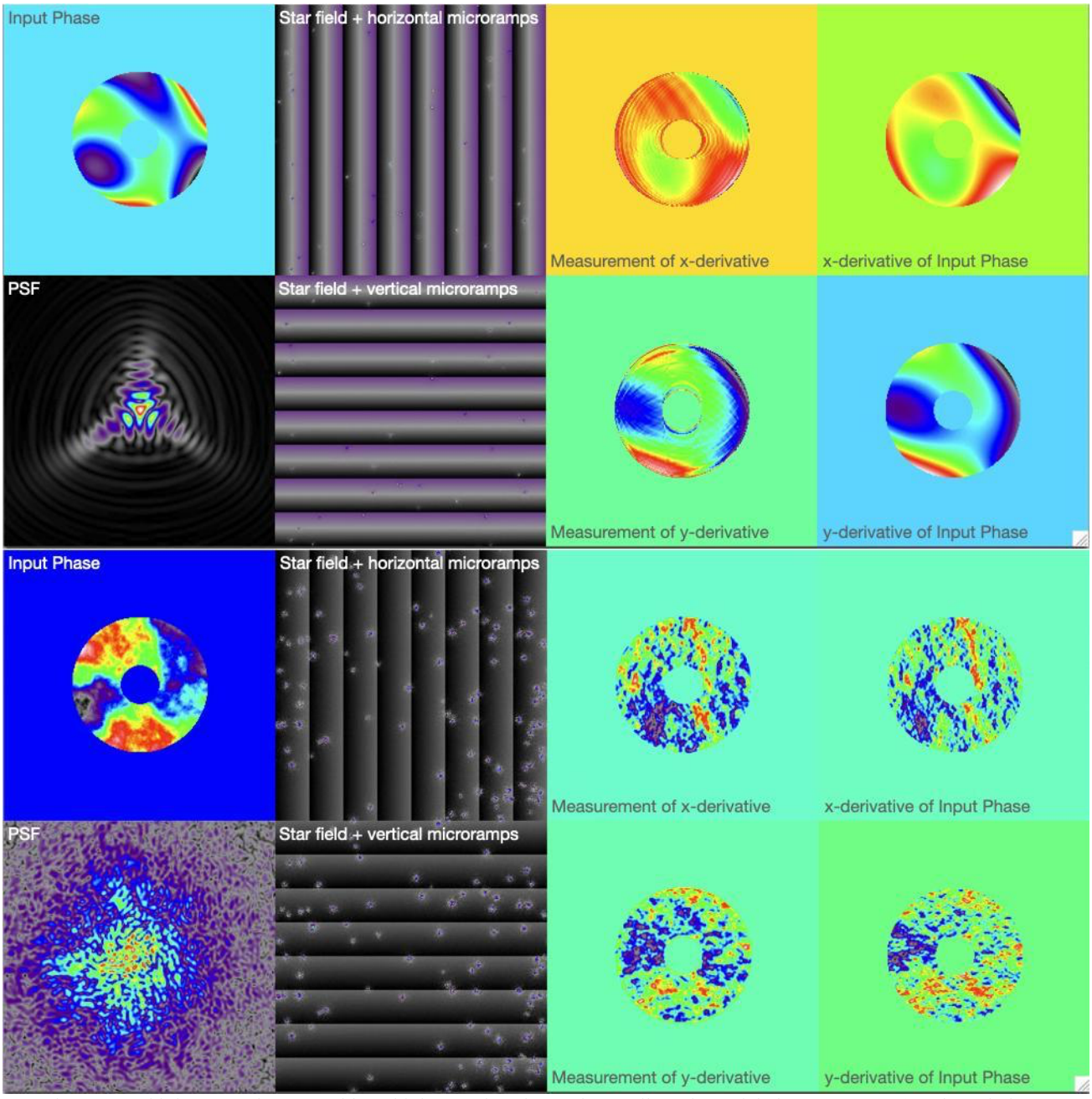

Figure 3: multiple sawtooth ramps with multiple stars for a low order zernike polynomial phase screen (top) and a turbulent phase screen (bottom); the rightmost column show the horizontal and vertical derivatives of the input phase (top left), and the column to the left of it shows the reconstructed phase derivatives.

2.3 Deformable mirror concepts

One of the constraints of GLAO is the conjugation of the deformable mirror with the pupil of the telescope and in traditional pupil reimaging systems, this requires large transfer optics. On a small telescope, this constraint is somewhat relaxed, and transmissive phase corrector such as deformable lenses developed by Dynamic Optics in Italy (Quintavalla et al., 2020 [8]), or spatial light modulators, would allow a relatively simple on-axis design. The adaptive lenses are cheap and fast but have a limited number of degrees of freedom, while SLM are usually slower and chromatic. We have not studied these trade-offs further, as ideally, we would prefer to avoid relay optics if possible. We recognize that having an "AO box" that can be mounted at a Cassegrain focus might be desirable, so we will investigate such options in the future.

For the time being, with the advent of new actuator technologies enabling large convex deformable mirrors, adaptive secondary mirrors are now becoming a reality, tremendously simplifying the implementation of GLAO, which becomes integrated to the telescope (Kuiper et al., 2020 [6]). The deformable mirror will still be misconjugated with respect to the ground layer (at negative altitudes, i.e. below the ground) for a Cassegrain design, but for 1-2m class telescopes the misconjugation is not large (on the order of 20 meters for the UH 2.2m telescope). If this turns out to affect performance, this could be alleviated by a Gregorian design.

Due to the thickness of the boundary layer, there will be some blurring of the phase over the field of view, which will set the optimal number of actuators on the deformable mirror. The number of actuators is an important parameter as it directly impacts the hardware cost. The optimal number will depend not only on the thickness of the boundary layer, but also the field size, the imaging wavelength, and the strength of the free atmosphere turbulence, which will impose the minimum allowable residual phase error. But it is also important to not undersize the actuator count, as conditions change and ideally the system would be designed to take advantage of the best observing conditions. The number of actuators can be roughly estimated from geometrical considerations (e.g., Tokovinin's "grey zone") and an error budget, but the exact performance requires simulations to properly be able to predict the gain in image quality, as the GLAO PSF has a specific morphology, with a sharper core but broadened wings. As an order of magnitude, adaptive secondary mirrors will require between 50 and 500 actuators on a diameter between 10 and 40cm, depending on the telescope diameter, the wavelength of operation and the desired level of performance.

3. SIMULATIONS AND ASSOCIATED PERFORMANCE PREDICTION

We have developed a Monte Carlo simulation code which takes into account the main components of an idealized system; it consists of a star field, a simple two-layer atmosphere, a physical optics model of the wavefront sensor, a synthetic deformable mirror and a simple integrator closed loop correction. The star field was generated from the Besançon Model at the North Galactic pole, although we varied both its density and its brightness in different cases: the North Galactic Pole is the worst possible case in terms of star density and brightness, and we know we can expect better performance closer to the galactic plane. The atmosphere was simulated with one layer at the ground and the other at an altitude where the meta-pupil starts to become discontinuous (i.e. the top of the "grey zone") and we ran cases for bad (r_0=0.07m) and good seeing (r_0=0.2m) with an optimistic profile with 75% of the turbulence in the Ground Layer (r_{0_GL}=0.24m and r_{0_FA}=0.45m for the good seeing case and r_{0_GL}=0.08m and r_{0_FA}=0.16m for the bad seeing case). The wavefront sensing was carried out at a wavelength of 500nm and in all cases, each of the four pupil subimages were 20x20 pixels across the pupil diameter, with no read noise (but photon noise included, with a zero-point of 1000 photons/sec/cm^2/Å for a magnitude 0 star). The quantum efficiency (QE) of the detector and throughput for the wavefront sensor (WFS) was optimistically set to 0.8 and the WFS sampling frequency was arbitrarily chosen to be 500Hz for a wind speed of 10m/s in the ground layer and 50m/s in the free atmosphere; the sampling frequency should be optimized as with the current settings, the ground layer moves by 1/5th of a subaperture in one integration time and the servo-lag error can probably be increased without decreasing the performance, although this will depend on the imaging wavelength. Slowing down the loop will help improve the sensitivity which is equivalent (if the servo-lag error remains negligible) to multiplying the star flux by a constant (see below).

The program first determines the optimal offset to avoid having bright stars at or near a sharp edge of the ramp mask; it then computes an interaction matrix between the deformable mirror and the wavefront sensor and inverts it. Finally, it runs the closed loop for 2000 iterations to average the speckle noise and provide a long exposure PSF.

We ran the closed loop simulations for two example cases:

- A 1m class telescope using a 11x11 deformable mirror and,

- A 2.2m telescope using a 21x21 deformable mirror.

For the 1m telescope we used a 30' field but we increased the star density (by scaling the field by a factor 2). For the 2.2m telescope we used a 40' with the NGP distribution. We also ran both cases but with the flux multiplied by a factor 4 (~$5x10^4$ photons per WFS subimage for the 1m telescope and 10^5 photons for the 2.2m case) to establish a performance baseline where photon noise would not be a limiting factor, as well as with the true NGP flux. We computed Strehl and FWHM on the long exposure PSFs for all the stars in the field at different wavelengths (500 and 700nm for the 1m telescope and 700nm, 1.0 and 1.5µm for the 2.2m telescope).

3.1 2.2m telescope simulation results

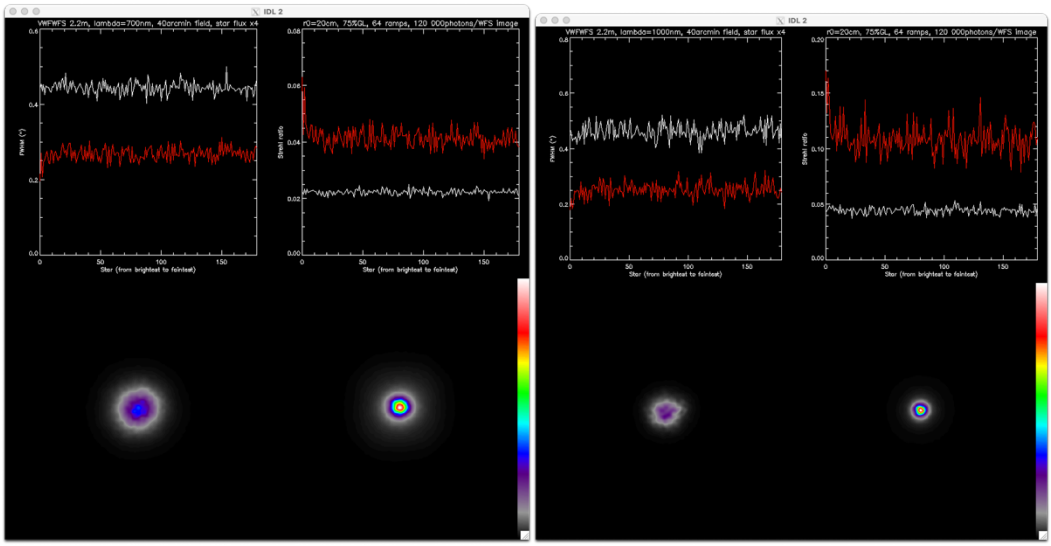

Figure 4(a): FWHM and Strehl with (red) and without (white) AO correction on 2.2m telescope, North Galactic Pole 40' field (but with star flux x4), 120 000 ph/WFS subimage. DM=21x21, r0=0.2m (2 layer atmosphere with 75% in ground layer), 64 ramps, 2000 iterations. 500nm wavefront sensing wavelength, 700nm (left); 1µm (right) imaging wavelength. The x-axis is the star number, arranged by decreasing brightness.

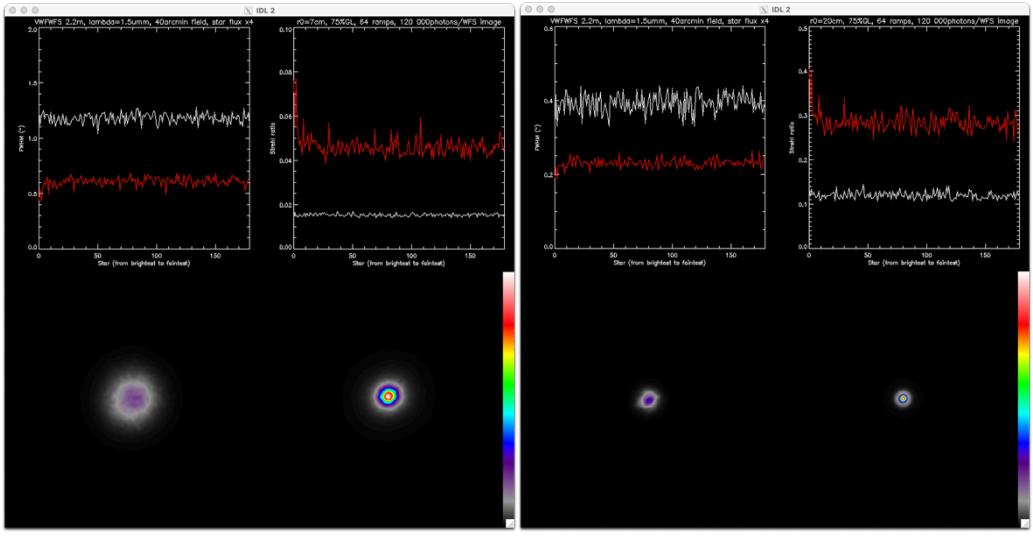

Figure 4(b): FWHM and Strehl with (red) and without (white) AO correction on 2.2m telescope, North Galactic Pole 40' field (but with star flux x4), 120 000 ph/WFS subimage. DM=21x21, r0=0.07m (left) and r0=0.2m (right) with a 2 layer atmosphere with 75% in a ground layer. 64 ramps, 2000 iterations; 500nm wavefront sensing wavelength, 1.5µm imaging wavelength.

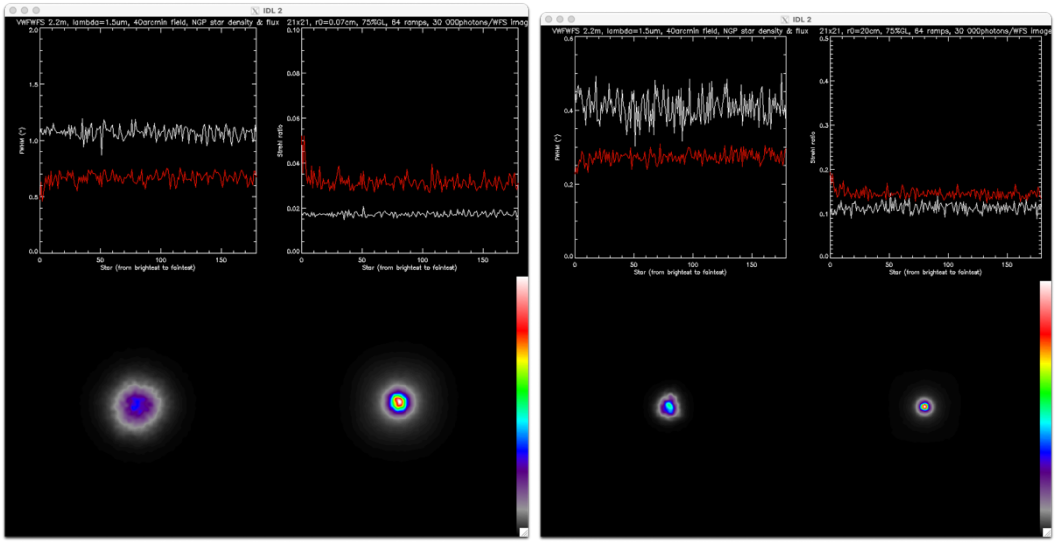

Figure 4(c): same as Figure 4(b) but with NGP star density and fluxes, 180 stars with magnitudes ranging from 10.4 to 18, yielding 30000 photons per WFS image. r0=0.07m (right) and r0=0.2m (right).

Compellingly, results for the 2.2m telescope show that it is almost possible to achieve the diffraction limit of the telescope at H band (0.15" at 1.5µm) over the entire field under good seeing conditions (r_0=0.2m) and that the resolution remains at the 0.2" level down to almost 700nm (although this will of course depend on the actual turbulence profile and strength of the free atmosphere seeing). This performance is achievable when the number of photons per WFS sub-image per integration time is >100 000 (since there are 20x20 pixels in each sub-images, this is coherent with the notion that the performance is not limited by photon noise when SNR/pixel>10), but even with the most unfavorable conditions of North Galactic Pole star densities and fluxes, there is still some gain in performance as shown in Figure 4(c).

3.2 1m telescope simulation results

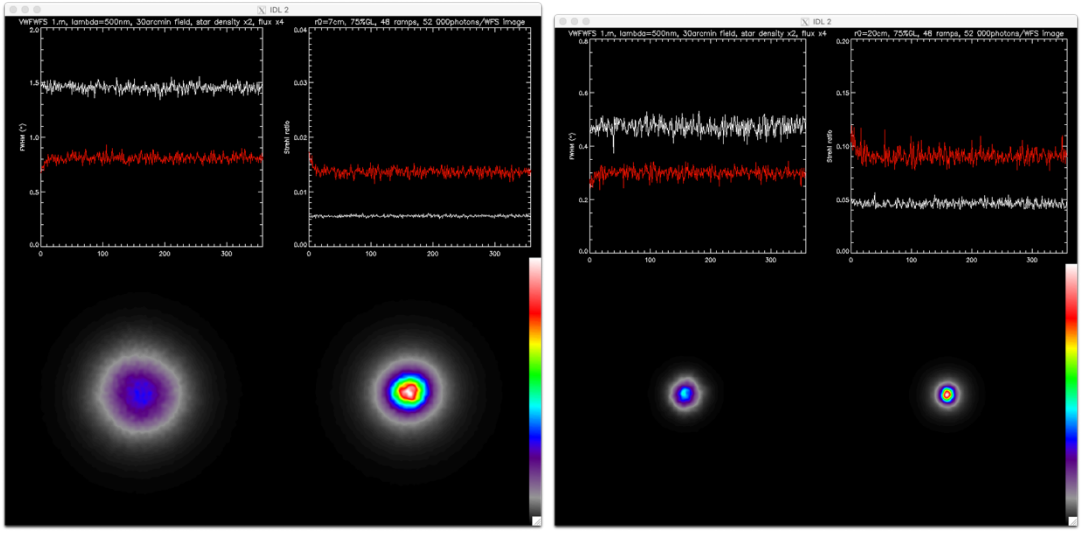

Figure 5(a): 1-m telescope, 11x11 DM, r0=7cm (left), r0=20cm (right) with 75% ground layer turbulence. Field=30' (star density NGPx4), 48 ramps, 52 000 photons per 20x20 subimage, 2000 iterations. 500nm imaging and wavefront sensing wavelength.

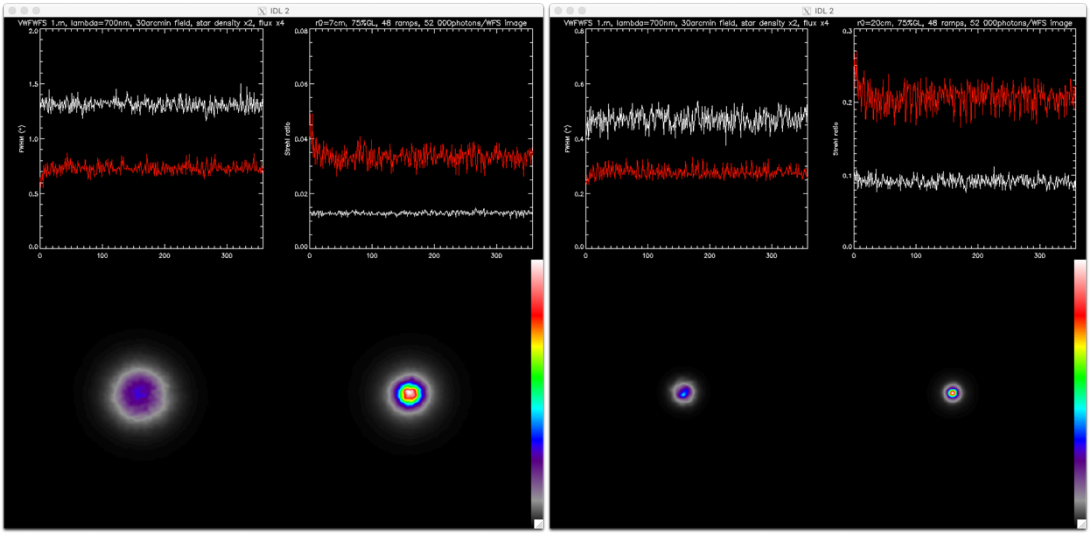

Figure 5(b): 1-m telescope, 11x11 DM, r0=7cm (left), r0=20cm (right). Field=30' (star density NGPx4), 32 ramps,52 000 photons per 20x20 subimage, 2000 iterations. Wavefront sensing wavelength=500nm, imaging wavelength=700nm.

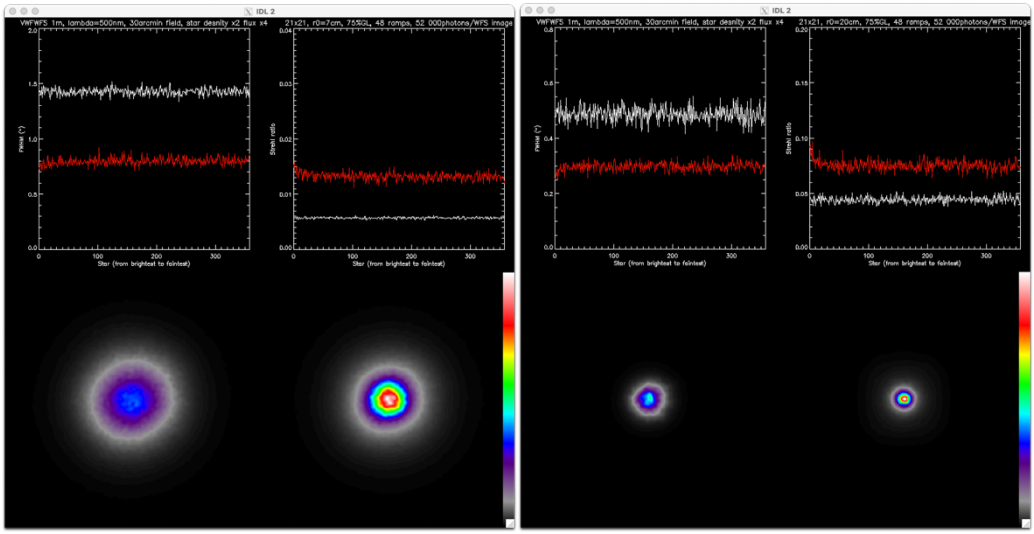

Figure 5(c): 1m telescope with 21x21 DM but all other parameters are the same as Figure 5(a), illustrating that a very high order system does not improve performance when it is limited by the free atmosphere seeing.

We find that in all cases, it is reasonable to expect a gain of a factor ~2 in both FWHM and in Strehl ratio. This is true even when the seeing is bad, which is important for amateur telescopes which may be deployed in suboptimal conditions. However, in cases of good seeing at longer wavelengths, diffraction limited performance is achievable, when the free atmosphere turbulence allows it.

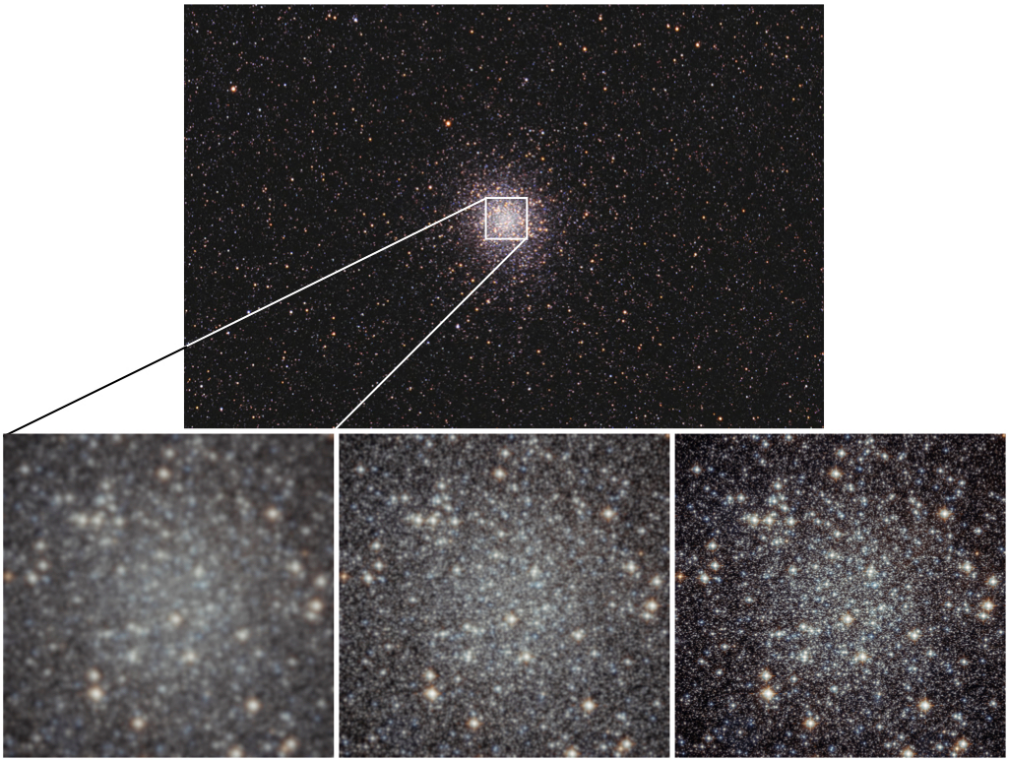

Figure 6: Wide field image of Messier 22 obtained from ground (top). Bottom right, highest resolution (0.07") image of the core of M22 obtained by Hubble Space Telescope, with a 3.5'x3.5' field. Bottom left, we have degraded the HST image of the core of M22 to approximately match a good ground based observing site (~0.5"), and in the middle we have improved it by a factor 2 in FWHM (~0.25"), as one might expect from the wide field AO correction results of figure 5(b) right.

4. NOMINAL INSTRUMENT DESIGN

4.1 VWFWFS: Very Wide Field WaveFront sensor

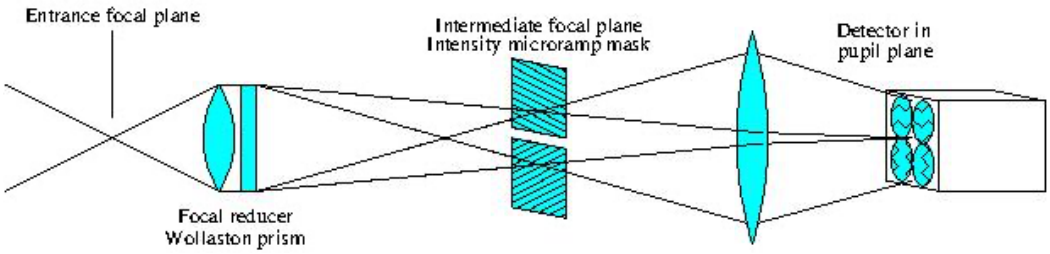

Figure 7: conceptual layout of the VWFWFS. The beam is split in two and each beam is focused on the micro-ramp arrays in a focal plane. The light from the entire field for each beam is then collected and an image of the pupil is formed on a camera (at the right).

The concept of the very wide field wavefront sensor requires inserting a focal plane mask and then reimaging the associated pupil image (or images) as shown in Figure 7. In practice, two masks are needed, one for the horizontal ramps (generating the vertical derivative) and one for the vertical ramps (for the horizontal derivative of the wavefront). Furthermore, each ramp is a transmission ramp, so unless the ramps are made to be gradually semi-reflective (and the reflected and transmitted light are collected), half of the light will be lost. An elegant solution exists to use all the light for the wavefront sensing, by using polarising optics where each linear polarisation is used for the horizontal/vertical images and the focal plane masks have polarisation gradients to transmit the ramp and the (1-ramp) images: Polarizing optics allow the optimal use

all the available light (see Figure 8). However, custom polarizing optics are not cheap, and these would need to be large format.

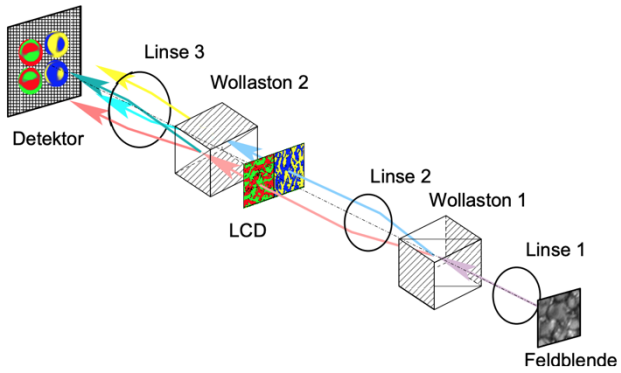

Figure 8: schematic layout of a polarisation optics based wide field wavefront sensor (from D. Schmidt, Ph.D. Thesis, 2006 [14]). The field is split in two by Wollaston 1. The microramps are gradual linear polarisation masks illustrated in blue/yellow and green/red for horizontal and vertical. Each polarisation is then separated again by Wollaston 2 to generate the 4 pupil images on the detektor.

Thus, there is a trade-off in the size of the field for the wavefront sensor:

- A large field improves the sky coverage by increasing the amount of flux sent to the pupil images of the wavefront sensor and improves the GLAO correction and uniformity by better averaging the ground layer turbulence.
- However, a large field also requires larger optics, thereby increasing the cost and decreasing the sturdiness of the wavefront sensor.
- The optimal field size may also depend on the telescope size and the application.

For example, for a 1m class telescope aimed at astrophotography, 100% sky coverage may not be necessary, since many interesting fields and nebulae can be found near the galactic plane with high star densities. Commercially available large format detectors for amateur telescopes have detectors with ~10000^2 pixels (e.g., ZWO ASI6200MM, based on Sony IMX455 CMOS with 9576x6388 pixels of 3.76µm retails for $4000) would cover a field of 13x10 arcminutes with 0.1” pixels (7m focal length, F/D=7, 43.4mm field diagonal); thus, for such a system, a 10-arcminute field of view for the wavefront sensor may be more than adequate. However, for a professional general use telescope in the 2m class, sky coverage may be more important and larger fields could justify the extra expense and complexity associated with larger optics. An important consideration is whether the F-ratio of the wavefront sensor should be different than that of the science beam: a focal reducer could be used in the wavefront sensor to miniaturize the field size (as long as the microramps can be miniaturized as well) without introducing detrimental aberrations; on a 2.2m telescope at F/10, a 40 arcminute field of view measures 0.25m, which is too large for any reasonable optical layout.

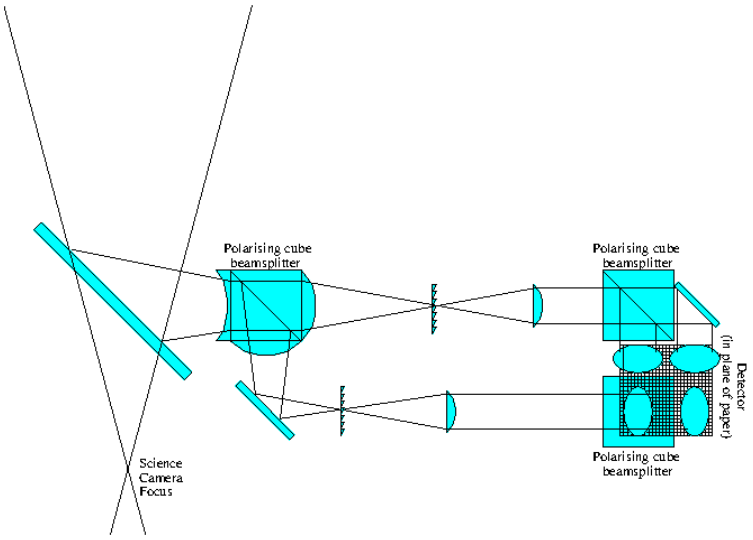

Figure 9: Sketch of possible layout for VWFWFS using polarizing beam splitter cubes (which could be replaced by Wollaston prisms if length for beam separation is not too long). Each focal plane has its own micro ramp and "transmitted" and "reflected" beams are again separated by another beam splitter cube. The four pupil images are imaged on the same detector. The size of the optics (and of the general layout) is determined by the size of the pixels in the wavefront sensor and the size of the micro ramp arrays. Care will need to be taken that each beam has the same distance to the detector (not shown in this sketch); additional folds may be required.

We note that for a laboratory experiment and a proof-of-concept on-sky demonstrator, the field does not need to be large, and we may even be able to demonstrate the principle in a simplified dual pupil image version (one for horizontal, one for vertical, using only the "transmitted" beam and normalizing by a synthetic uniform illumination pupil).

4.2 Practical considerations

Real world implantation of the VWFWFS concept faces three main challenges:

- Sky background photon noise. For the very darkest sky (no moon, excellent site, no light pollution) the magnitude of the night sky is about 22mag/arcsec^2 while 18mag/arcsec^2 may be a more reasonable value for a rural/suburban sky. Using a zero point of 1000 photons/cm^2/sec/Å), and the same QE, sampling frequency and bandpass as in the simulations below, we can estimate the number of photons contributed by stars and the sky to the WFS images; To obtain reasonable closed loop performance, a 1-m telescope required about 5x10^4 photons per WFS sub-image and ~10^5 for a 2-m telescope. The number of photons for the different telescopes and different field sizes is given in the table below:

Sky Magnitude	22	18
1-m telescope (10')	9000	3.5x10^5
1-m telescope(30')	8x10^4	3.2x10^6
2-m telescope (10')	4x10^4	1.7x10^6
2-m telescope (30')	3.9x10^5	1.5x10^7

In the darkest possible skies and a small field of view, the contribution of the sky background is tolerable, but can easily become dominating in less-than-ideal conditions. Some form of active filtering of this light will be required for practical implementation.

- Custom polarizing optics can be expensive: the price of a 2.5cmx2.5cm component is on the order of k€20, and for a 5cmx5cm component (which is the largest size that can be manufactured), the cost would be on the order of

k€50. As two are needed for the horizontal and vertical derivatives, the cost in custom optics would be on the order of k€100.

- Optical design: for the pupil images of each star to line up on the detector, the optical design must be telecentric. Furthermore, the large field of view imposes constraints on the size of the optics: The Lagrange invariant is the product of the beam size and the angle of the paraxial ray and is conserved throughout the optical system. A large field at small F-number will produce very large angles on the pupil image if the pupil image is smaller than the field image. This is less stringent for smaller fields but may become an optical design constraint for larger telescopes with larger fields.

Due to these issues (cost of custom optics, the size of the optical layout and the sky background), we must consider two approaches for the implementation of the VWFWFS: For 1-m class telescopes, we favor simplifying the concept at the expense of performance and sky coverage to keep the cost down, whereas for the >2m class telescope, performance and sky coverage justify the added complexity and higher cost.

4.3 Cost-effective VWFWFS for 1m class telescopes

Considering the cost of custom optics as well as the need to reduce sky background, we propose a simplified version of the VWFWFS using only one pupil image per horizontal and vertical derivative and a simple addressable transmissive LCD screen. The transmission pattern on the screen is dark everywhere apart from at the locations of stars in the field, where a knife edge pattern is imposed on each star to generate the optical differentiation signal in the pupil. Commercially available transmission screens are available with sufficient resolution at low cost (e.g. Holoeye LC2012 provides XGA resolution (1024x768) for ~k€2). If the field of view of the VWFWFS is 10', then each pixel is 0.6" on sky, so for typical 1" seeing, we can place a knife edge with half of the FWHM of each star. Half of the light is lost, and the smaller field of view also affects the sky coverage and the performance in sparse areas of the sky, but the components are readily available, and the layout are simple. The Holoeye LC2012 measures 37mmx28mm, which requires a focal length of 5.7m to cover 10' on sky, so the wavefront sensor's entrance F-ratio is 5.6, compatible with standard Cassegrain configuration for this class of telescopes (a small focal reducer may be required). A strawman design is depicted in Figure 10.

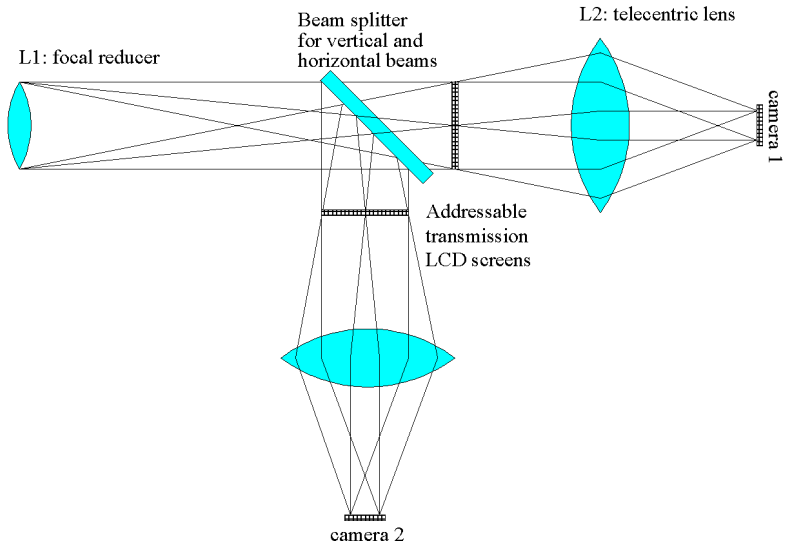

Figure 10: Strawman design for basic VWFWFS implementation. See text for details.

L1 is a focal reducer and with L2, it reimages the field at infinity, seen from the camera, making the beam telecentric. Addressable transmission LCD screens are placed in the focal planes for each of the horizontal and vertical derivative beams, with a size of 35mm. The distance between the focal plane and L2 determines the size of the pupil reimage on the cameras; if the size of the pupil on the camera is e.g., 2mm, the distance of L2 from the focal plane is only 11.2mm, so a reimaging optic may be required reduce the pupil image size. Unfortunately, this compact design requires two cameras as it appears difficult to fold the beams back on a single camera.

4.4 Deformable mirrors and telescope integration

The use of an adaptive secondary mirror implies using a Cassegrain, Gregorian or Nasmyth focus. The drawback of the Nasmyth focus is that the field (and therefore the focal plane masks) must rotate with respect to the telescope to account for changes in elevation (or declination on an equatorial mount). The wavefront sensor has a natural position at the Cassegrain focus, although what is gained with respect to field rotation now translates into stiffness requirements to avoid flexures, since the wavefront sensor may be sizable for large fields. However, to keep in line with the project philosophy, we think it is preferable to avoid field rotation compensation and focus on a stiff WFS structure. Also keeping the wavefront sensor close to the science camera (Figure 9) ensures that differential flexures can be minimized.

The imaka wide-field GLAO demonstrator on the UH88 telescope on Maunakea is currently being equipped with a 600mm adaptive secondary mirror with 211 actuators. It will be controlled in GLAO mode by 5 fixed wavefront sensors, as in the current imaka system, since there will be no need for an optical relay to re-image the pupil, the pickoffs will be at the direct Cassegrain focal plane of the telescope. This would be an ideal platform to demonstrate the VWFWFS concept and would also allow to use imaka for general purpose wide-field high angular resolution observing, as it would essentially provide 100% sky coverage. We are also considering the possibility of demonstrating this wavefront sensing technique on the C2PU 1-meter telescope at Observatoire de la Côte d'Azur in Calern, where we already have an adaptive optics demonstrator bench with a 1' field of view, and where we have demonstrated the use of deformable lenses (Quintavalla et al., 2020 [8]).

5. CONCLUSIONS AND FUTURE WORK

We have presented a concept to implement adaptive optics with substantial sky coverage for telescopes in the 1-2m class. We believe there is an interesting and unique case for these telescopes, although the applications may have substantial impact on the details of the implementation. Some remaining aspects still require further research, some of which are application dependent, while others are more general optimisation issues:

- Simulations to optimize the number/size of the ramps and optimize performance.
- Use (and cost) of polarizing optics for optical design,
- optical layout as a function of field size and other technical choices (optical quality requirement for WFS optics).
- Identify possible detector for VWFWFS (few pixels, very low read noise).

Adaptive secondary mirrors are becoming available for smaller telescopes using a new actuator technology developed by TNO. A lab demonstrator is currently being planned and telescope tests are being considered for the C2PU 1m telescope and the UH-2.2m imaka AO system.

Simulations show that good sky coverage is possible with a 30' field on a 1m telescope, but large fields require large optics, and the optimal field size depends on the telescope size and the application. For a 1m class telescope aimed at astrophotography, 100% sky coverage may not be necessary, since many interesting fields and nebulae can be found near the galactic plane with high star densities. Commercially available large format detectors for amateur telescopes can cover fields of 10x10 arcminutes with 0.1" pixels; thus, for such a system, a 10-arcminute field of view for the wavefront sensor may be more than adequate and only needs a small number of pixels (40x40) read out at 500Hz.

The motivation to develop compact and robust AO system for small telescopes is two-fold: On the one hand, schools and universities often have access to small telescopes as part of their education programs. Also, researchers in countries with fewer resources could also benefit from well-engineered and reliable adaptive optics on smaller telescopes for research and education purposes. On the other hand, amateur astronomers and enthusiasts want improved image quality for visual observation and astrophotography. Implementing readily accessible adaptive optics in astronomy clubs would also likely have a significant impact on citizen science.

REFERENCES

[1] Abdurrahman, F., Lu, J., Chun, M., Service, M., Lai, O., Föhring, D., Toomey, D., Baranec, C., "Improved Image Quality over 10· Fields with the ´Imaka Ground-layer Adaptive Optics Experiment", *The Astronomical Journal* (2018), **156**, 100.

[2] Babcock, H.W., "The Possibility of Compensating Astronomical Seeing." *Publications of the Astronomical Society of the Pacific* **65**, 229 (1953).

[3] Dauvergne J.-L., Dovillaire G., Colas F., Delcroix M., Lecacheux J., Rondeau C., Juval R., 2018, EPSC abstracts Vol 12. https://media.afastronomie.fr/RCE/PresentationsRCE2018/Dauvergne-RCE2018.pdf

[4] Fauvarque, O., Neichel, B., Fusco, T., Sauvage, J.-F., Girault, O., "General formalism for Fourier-based wave front sensing: application to the pyramid wave front sensors", *Journal of Astronomical Telescopes, Instruments, and Systems*, **3**, 019001 (2017)

[5] Hafftert, S., "Generalised optical differentiation wavefront sensor: a sensitive high dynamic range wavefront sensor", *Optics Express* **24**, p.18986-19007 (2016)

[6] Kuiper, S., Jonker, W. A., Maniscalco, M., van der Ven, E., Voorhoeve, R., Chun, M., Lai, O., Lu, J., "Performance analysis of the adaptive secondary mirror for the UH2.2 telescope", Proceedings of SPIE **11448**, 114485R (2020)

[7] Loktev, M., Vdovin, G., Soloviev, O., "Integrated adaptive optics system for small telescopes", Proceedings of SPIE, 2008 vol. 7015. 7015.

[8] Qunitavalla, M., Spagnol, M., Abe, L., Carbillet, M., Aristidi, E., Mocci, J., Muradore, R, Bonora, S., "XSAO : an extremely small adaptive optics module for small aperture telescopes with multiactuator adaptive lens", *JATIS*, **6**, 029004 (2020).

[9] Ragazzoni, R. "Pupil plane wavefront sensing with an oscillating prism", *Journal Modern Optics*, **43**, 289 (1996)

[10] Ragazzoni, R., "Multiple field of view layer-oriented adaptive optics. Nearly whole sky coverage on 8 m class telescopes and beyond", *A&A*, **396**, p.731-744 (2002)

[11] Rigaut, F., "Ground Conjugate Wide Field Adaptive Optics for the ELTs." *Beyond conventional adaptive optics*, 2002, European Southern Observatory Conference and Workshop Proceedings 58, 11.

[12] Roddier, F., "Curvature sensing and compensation: a new concept in adaptive optics." *Applied Optics* **27**, 1223–1225. (1988)

[13] Roddier, F., "Adaptive optics in astronomy", edited by Francois Roddier. Cambridge University Press, 1999, ISBN 052155375X

[14] Schmidt, R., "Testaufbau eines neuen Sensors zur Bestimmung der Wellenfrontdeformation in optischen Sonnenteleskopen", Ph.D. Dissertation, University of Freiburg, 2006.

[15] Schmidt, D., von der Lühe, O., "Optical wavefront differentiation: wavefront sensing for solar adaptive optics based on a LCD", Proceedings SPIE *Adaptive Optics for Laser Systems and Other Applications* **6584**, 658408 (2007)

[16] Stuik, R., Bacon, R., Conzelmann, R., Delabre, B., Fedrigo, E., Hubin, N., Le Louarn, M., Ströbele, S., "GALACSI The ground layer adaptive optics system for MUSE", *New Astronomy Reviews*, **49**, 618-624 (2006)

[17] Tokovinin, A., "Seeing Improvement with Ground-Layer Adaptive Optics." *Publications of the Astronomical Society of the Pacific* **116**, 941–951. (2004)